

Performance of adding waste glass and sewage sludge to reservoir-sediment aggregates

Ing-Jia Chiou^{*1}, Chin-Ho Chen^{2b} and Chia-Ling Lin¹

¹Graduate School of Materials Applied Technology, Department of Environmental Technology and Management, Taoyuan Innovation Institute of Technology, No. 414, Sec. 3, Zhongshan E. Rd., Jhongli, Taoyuan 320, Taiwan, ROC

²Department of Social and Regional Development, National Taipei University of Education, No. 134, Sec. 2, Heping E. Rd., Taipei City 106, Taiwan, ROC

(Received March 18, 2013, Revised August 5, 2013, Accepted August 31, 2013)

Abstract. Accumulated annual reservoir sedimentation in Taiwan was 14.6 million m³ in 2010, seriously endangering reservoir safety and the water supply. In addition, the sintering temperature of reservoir-sediment aggregates (RSAs) is very high, and very energy consuming consequently. Therefore, to explore the effects of admixtures on sintering behavior and performance of the aggregates, two different admixtures are blended, waste-glass and municipal sewage sludge, into reservoir sediment to make artificial aggregates. Experimental results show that the lightweight characteristics of waste-glass/reservoir-sediment aggregates (WGRSAs) are more significant than those of sewage sludge/reservoir-sediment aggregates (SSRSAs). Moreover, as sintering temperature increases, the specific gravity of WGRSAs drops more apparently. The optimum sintering temperature of pure reservoir-sediment aggregates (PRSAs), SSRSAs, and WGRSAs was 1150°C, 1100°C, and 1050°C, respectively. The PRSAs are normal weight with better strength; the WGRSAs are lightweight and energy-saving; and the SSRSAs are lightweight with normal strength.

Keywords: reservoir sediment; admixture; artificial aggregate; lightweight, sinter

1. Introduction

According to investigations conducted by the Water Resources Agency, Ministry of Economic Affairs, nearly 70 reservoirs in Taiwan have serious sediment problems. Total sedimentation was estimated at about 470 million m³ in 2010, while the annual increase in sediment load is about 14.6 million m³. Clearly, reservoir sedimentation problems are very serious and reservoirs need to be dredged. Most reservoir sediment (RS) is simple sediment, comprised of Illite and Chlorite, which are similar to silt or clay (Hung and Hwang 2007, Chiou and Chen 2013). Therefore, RS is very suitable as a substitute for clay. In addition to lightweight aggregates, RS could be utilized as fill, cement, brick, artificial reefs, wave absorption blocks, and slope protection blocks.

*Corresponding author, Associate Professor, E-mail: cij@tiit.edu.tw

^aPh.D., E-mail: cij@tiit.edu.tw

^bProfessor., E-mail: chchen@tea.ntue.edu.tw

In recent years, technology for producing artificial aggregates typically uses waste as a substitute for traditional clay materials. Industrial waste heat is often converted into useful energy. A comprehensive survey of Europe, the United States, Japan and other advanced countries indicates that *ocean disposal of* waste sludge *has been* forbidden, the fraction of landfills has been significantly reduced, and heat-treatment technology has become increasingly important, as are applications in energy, agriculture, and recycling materials (Chiou *et al.* 2006). The recycling applications for municipal sewage sludge are agricultural soil improvement (Khan and Scullion 2002, Singh and Agrawal 2008), porous materials or lightweight composite materials (Wang *et al.* 2005), lightweight aggregates (Chiou *et al.* 2006, Cheeseman and Viridi 2005, Wang *et al.* 2009, Chiou and Chen 2011), lightweight aggregates and non-structural concrete (Mun 2007, Wang and Sheen 2010), and ceramics (Qi *et al.* 2010). As it contains particularly rich organic matter, sewage sludge (SS) can be used as a composition adjusting agent when producing lightweight aggregates (Chiou *et al.* 2006, Chiou and Chen 2011). Annual SS yield in Taiwan is about 0.5 million tons, and the penetration rate of public sewer system has improved yearly. Hence, the amount of SS will increase, such that reducing the amount of sewage sludge and implementing recycling measures are now very important. Additionally, according to Taiwan's Environmental Protection Administration (EPA), approximately 211,600 tons of waste glass (WG) containers were recycled in 2010 in Taiwan. The applications of recycled waste glass included concrete aggregates (Park *et al.* 2004, Corinaldesi *et al.* 2005, Terro 2006, Ismail and AL-Hashmi 2006), recycled glass or glass ceramics (Yu`ru`yen, Toplan 2009, Bernardo *et al.* 2010, Zhang *et al.* 2011, Vu *et al.* 2011), artificial slates (Lee *et al.* 2008), pozzolanic materials (Lee *et al.* 2011, Lin *et al.* 2009), and lightweight aggregates (Chiou and Chen 2013, Tsai *et al.* 2006, Wei *et al.* 2011). Furthermore, using WG (particle size less 600 μm) can reduce the alkali silica reactivity of concrete (Lee *et al.* 2011).

Considering the high sintering temperature and high energy consumption of RSAs (Chiou and Chen 2013, Tang *et al.* 2011, Chen *et al.* 2012), SS as a composition adjusting agent (Chiou *et al.* 2006, Chiou and Chen 2011), and ability of waste glass to reduce the sintering temperature (Chiou and Chen 2013, Tsai *et al.* 2006), thus, this study uses two wastes, SS and WG, as admixtures to analyze the pelletization and pellet characteristics, physical and chemical properties, as well as the microstructures of aggregates to study how the admixtures impact RSAs' sintering behaviors and the performance.

2. Methodology

2.1 Experimental materials

In this study, Sediment from the Shi-men Reservoir in Taoyuan County, dewatered sludge cakes produced by Taipei Di-hua Wastewater Treatment Plant, and WG provided by the waste-glass recycling plant were used as raw materials. The RS and SS are processed through drying, primary screening (screening debris), crushing, grinding, and final screening, to obtain RS powder and SS powder, respectively, which passed through a #100 sieve (less 150 μm). The RS's moisture, ash, and combustible content were 32.38%, 63.93% and 3.69%, respectively. Additionally, according to the *Unified Soil Classification* System (USCS), the RS is mostly silts and clays; its clay content reached to 60%, silt content was approximately 38% and its specific

gravity was 2.73. The moisture, ash, and combustible content in SS were 77.27%, 6.96% and 15.77%, respectively. After crushed, ground, and screened, the recycled WG bottles became waste glass powder that passed through the #100 sieve (less 150 μm). Through the scanning electron microscope (SEM), it clearly showed that both RS powder and SS powder were homogeneous, and WG powder consisted of irregularly shaped particles.

2.2 Design of experiments

According to a previous experiment from our research term (Tsai *et al.* 2006, Chiou and Chen 2011, Chiou and Chen 2013), three mixing proportions: pure RS (RS100); 80% RS and 20% WG (RS80WG20); and 80% RS powder and 20% SS powder (RS80SS20) were used to produce pure RS aggregate (PRSAs), WG/RS aggregate (WGRSAs) and SS/RS aggregate (SSRSAs), respectively (Table 1). After these raw materials were uniformly mixed, water was added into the materials and they were stirred. They were then squeezed with extrusion equipment with a mesh of 10mm, and cut into 9-10 mm pellets and processed on a tilting turntable to make pellets become increasingly dense and round. Diameter of the tilting turntable machine is 600mm. Then, according to the utilization experience and trial-and-error method to set the rotation rate of the tilting turntable at 22 ± 2 rpm, with inclined angle 27° , and operation time 10 - 20 min. Next, the pellets were air dried and oven dried, and then sintered under temperatures of 1100°C, 1150°C, 1200°C, and 1050°C respectively for 10 minutes with a heating rate of 5°C/min (Chiou *et al.* 2006, Chiou and Chen 2011, Chiou and Chen 2013).

The analytical items for the raw materials, RS, SS, and WG, included three components, loss on ignition, chemical composition, thermo-gravimetric loss (by DTA/TGA, Perkin Elmer, TGA 7, to raise temperature to 1300°C at heating rate 10°C /min under oxygen atmosphere.), and microstructures (SEM, HITACHI SU1510). The analytical items for RSAs were particle sizes, weight changes before and after sintering, specific gravity, water absorption, failure point loading, Mohr hardness, chemical corrosion resistance, chemical soundness, potential alkali-silica reactivity (ASTM C289-94), appearances, and microstructures (SEM, HITACHI SU1510).

Table 1 Proportions and sintering conditions of reservoir-sediment aggregates

| Aggregate No. | Reservoir sediment ,RS (%) | Sewage sludge, SS (%) | Waste glass, WG (%) | Sintering temperature (°C) | Heating rate |
|---------------|----------------------------|-----------------------|---------------------|----------------------------|--------------|
| RS100 | 100 | - | - | 1050, 1100, | 5°C/min |
| RS80SS20 | 80 | 20 | - | 1150, 1200 | |
| RS80WG20 | 80 | - | 20 | | |

Table 2 Chemical compositions of raw materials

| Raw materials | SiO ₂ | Al ₂ O ₃ | Fe ₂ O ₃ | CaO + MgO | K ₂ O | Na ₂ O | SO ₃ | P ₂ O ₅ | LOI |
|--------------------|------------------|--------------------------------|--------------------------------|-----------|------------------|-------------------|-----------------|-------------------------------|------|
| Reservoir sediment | 60.9 | 25.2 | 5.55 | 0.92 | 3.49 | 1.22 | 0.34 | - | 17.7 |
| Sewage sludge | 36.2 | 14.4 | 9.15 | 9.47 | 2.49 | - | 11.0 | 15.0 | 56.4 |
| Waste glass | 74.0 | 6.01 | 0.33 | 9.66 | 0.83 | 8.23 | 0.20 | - | 1.23 |

Table 3 Total amount and leaching concentration of heavy metals in raw materials

| Raw materials | Total Metal (mg/kg) | | | | |
|--------------------------|--------------------------------------|---------------|---------------|---------------|--------------|
| | Cu | Zn | Pb | Cd | Cr |
| RS | 27.37 ± 1.12 | 176.2 ± 4.41 | 44.35 ± 0.02 | 3.61 ± 0.11 | N.D |
| SS | 256.7 ± 1.83 | 367.6 ± 0.42 | 67.55 ± 1.42 | 5.78 ± 0.13 | 576.1 ± 1.16 |
| WG | 62.62 ± 5.66 | 160.5 ± 7.71 | 79.51 ± 0.83 | 4.93 ± 0.30 | N.D |
| Raw materials | Leaching concentration (TCLP) (mg/L) | | | | |
| | Cu | Zn | Pb | Cd | Cr |
| RS | 0.271 ± 0.003 | 0.707 ± 0.022 | 0.065 ± 0.001 | 0.037 ± 0.001 | N.D |
| SS | 0.092 ± 0.001 | 3.564 ± 0.011 | 0.032 ± 0.005 | 0.037 ± 0.001 | N.D |
| WG | 0.705 ± 0.030 | 3.100 ± 0.011 | 1.150 ± 0.017 | 0.061 ± 0.001 | N.D |
| Regulatory Limits (mg/L) | 15.0 | - | 5.0 | 1.0 | 5.0 |

ND : Not detected

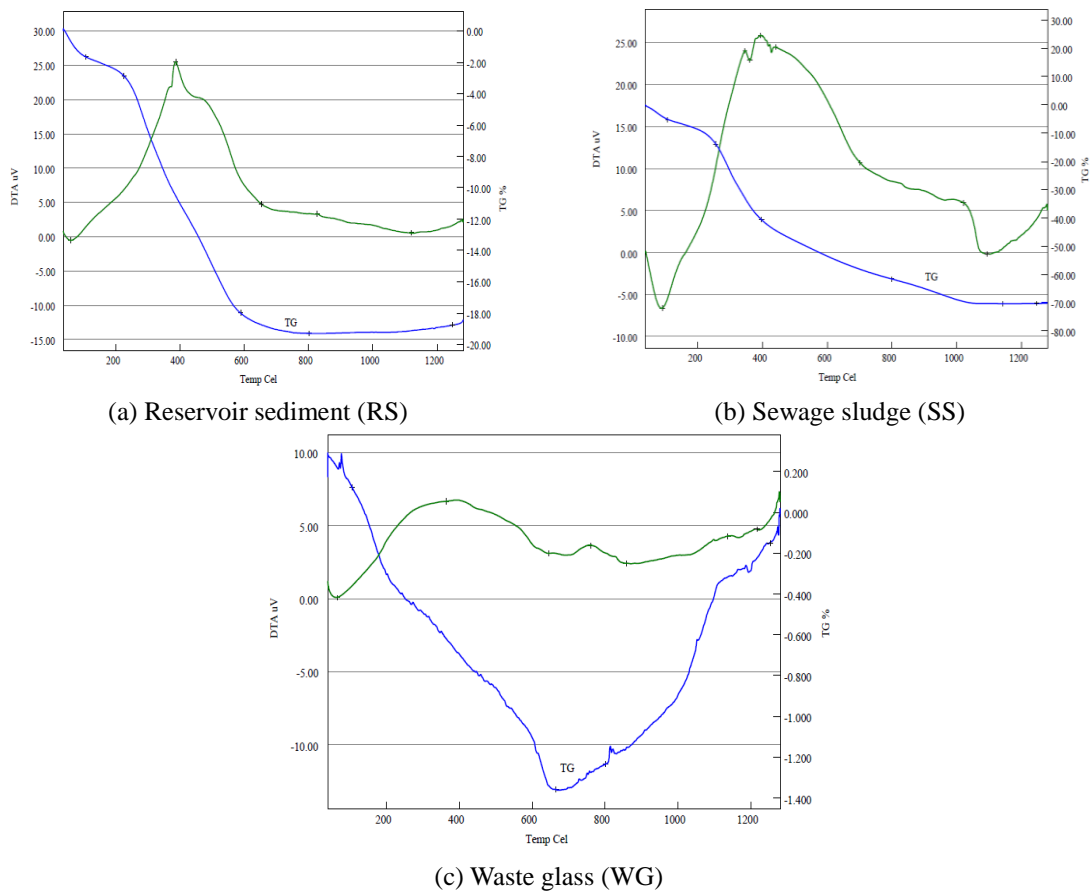


Fig. 1 DTA/TGA of raw materials

3. Results and discussion

3.1 Chemical compositions and thermal decomposition of raw materials

The chemical composition of RS is very similar to that of expansive clay, which is very suitable for producing RSAs. The RS contains 60.9% SiO₂, 25.2% Al₂O₃ and 5.55% Fe₂O₃. The SS contains rich organic substances and little grease. It contains 36.2% SiO₂, 15.0% P₂O₅, 14.4% Al₂O₃, 11.0% S₂O, and 9.15% Fe₂O₃. The WG contains up to 74.0% SiO₂, 9.66% CaO + MgO, 8.23% Na₂O, and 6.01% Al₂O₃ (Table 2).

Table 3 shows the total amounts of heavy metals and the leaching concentration in RS, WG powder, and SS powder. Fig. 1 shows the analytical results for thermo-gravimetric loss for RS, SS and WG. The RS had significant weight loss at 225–588°C, due to the organic matter volatilized and the exothermic peak occurred at 386°C. When the temperature was 588°C, weight loss was the most significant. At room temperature, SiO₂ in the RS was α -quartz. When the temperature was increased to 588°C, it changed from α -quartz to β -quartz. Maximum weight loss occurred at 801°C, and loss on ignition then was as high as 17.65%.

The SS had significant weight loss and its exothermic reaction at 255–396°C, as its organic matter volatilized. At 800–1144°C, the endothermic reaction and weight loss slowed, and its loss on ignition was 56.40%. An endothermic valley of WG powder occurred at 666°C, and its loss on ignition was 1.234%. According to its Thermogravimetric Curve (TG), when WG was heated to 802°C, weight loss was 1.11%, indicating that WG powder had better thermal stability.

3.2 Properties of reservoir-sediment mixed paste

The RS had a fine texture, classified as a kind of low-plasticity clay (CL). If the moisture content of clay is greater than the liquid limit, pellets will be formed easily but the paste has low cohesiveness; conversely, if the moisture content is less than the liquid limit, it will have difficulty forming pellets but the paste has high cohesiveness. Hence, pellets may have many cracks or micro-cracks. Therefore, the appropriate water consumption for RS100 paste is 38.9 wt% (Fig. 2). The SS is rich in organics matter, but loosely packed, and cannot absorb water easily because of containing some grease. The amount of SS used is positively correlated with the amount of water used in RS100, wherein water consumption of SSRSAs paste is 45.0 wt% (Fig. 2). The amount of WG used is negatively correlated with the amount of water used in the RS paste and water consumption of the WGRSAs paste is 28.75 wt%.

This study assessed the viscosity of freshly blended RS paste with fixed rotation speed of 300 rpm. Fig. 3 shows the torque value of the RS paste. With the same consistency, its torque value is 0.60kgf.cm, meaning that PRSAs paste has better plasticity and can be granulated easily to form a spherosome. Due to the high water absorption and loose structure of SSRSAs paste, the torque value of the paste decreased with the amount of blended SS increased. The torque value of SSRSAs paste is 0.30kgf.cm. However, when amount of SS blended is greater 30%, the pellets made of RSA paste typically deform due to their heavy weight. The torque value of WGRSAs paste is 0.70kgf.cm. When the viscosity of this paste increases, it is easier to form spherosome during granulation.

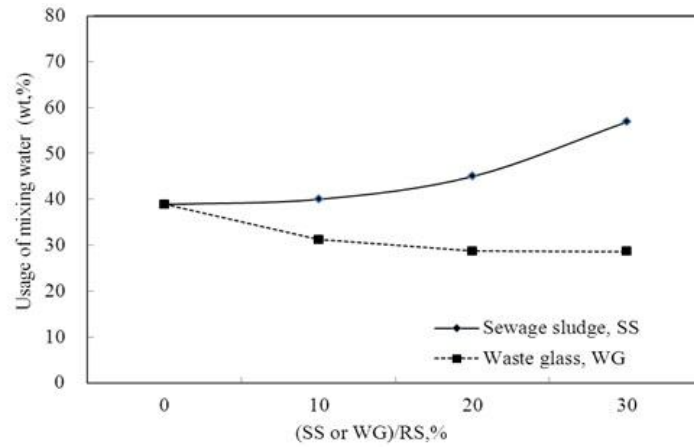


Fig. 2 Water usage of SSRSA paste and WGRSA paste

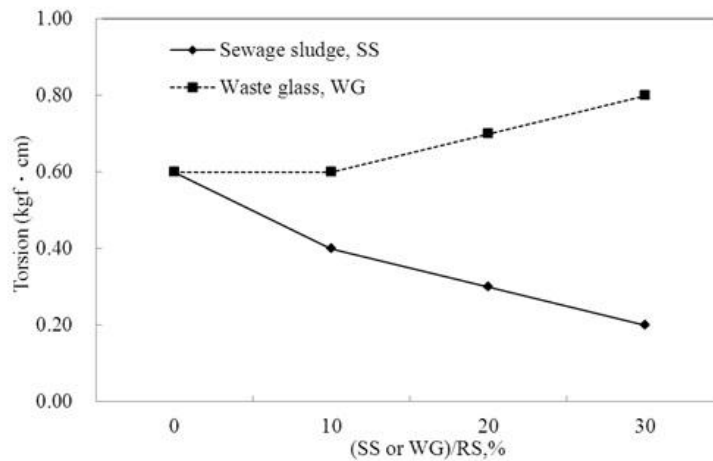


Fig. 3 Torsion of SSRSA paste and WGRSA paste

3.3 Particle size and weight change of reservoir-sediment aggregates before and after sintering process

The RSAs could not be sintered at 1050°C; however, at 1200°C, the RSAs would excessively melt flow and collapse. Thus, in this study, two sintering temperatures, 1100°C and 1150°C, were adopted. In each batch, 50 pellets of reservoir-sediment aggregates before sintering were randomly picked from the same mixing proportion, and measured their initial particle sizes in cross direction by electronic gauge. Then, the same 50 pellets of the same mixing proportion were sintered, and measured the particle sizes with the same way to calculate the particle size change before and after sintering. Table 4 shows the measurement results in particle size and weight change before and after sintering.

At 1100°C and 1150°C, the change rate in particle size of WGRSAs was -3.79 to -4.65% (shrinkage) and 5.68 to 6.30% (expansion) respectively; while the change rate in particle size of

Table 4 Particle size and weight change of reservoir-sediment aggregates before and after the sintering process

| Items | RS80WG20 | | RS80SS20 | |
|---|------------------|------------------|------------------|------------------|
| | 1100°C | 1150°C | 1100°C | 1150°C |
| D_{unsinter} (mm) | 13.21 ± 0.94 | 12.86 ± 0.85 | 13.58 ± 0.88 | 13.19 ± 0.81 |
| D_{sinter} (mm) | 12.71 ± 0.86 | 13.67 ± 0.81 | 11.57 ± 0.58 | 12.35 ± 0.72 |
| ρ_{unsinter} (g/cm ³) | 1.68 ± 0.24 | 1.57 ± 0.24 | 1.48 ± 0.16 | 1.43 ± 0.27 |
| ρ_{sinter} (g/cm ³) | 1.84 ± 0.24 | 1.23 ± 0.12 | 2.02 ± 0.23 | 1.50 ± 0.19 |
| $W_{\text{avg.}}$ (%) | -4.81 | -5.20 | -16.33 | -18.45 |
| $D_{\text{avg.}}$ (%) | -3.79~-4.65 | +5.68~+6.30 | -14.80~-18.33 | -6.37~-8.20 |
| $S_{\text{avg.}}$ (%) | -7.42~-9.08 | +11.67~+12.89 | -27.96~-33.36 | -12.30~-15.98 |
| $V_{\text{avg.}}$ (%) | -10.99~-13.36 | +17.95~+19.78 | -39.03~-45.62 | -17.92~-23.18 |
| $p_{\text{avg.}}$ (%) | +6.36~+9.52 | -19.77~-21.66 | +36.49~+52.63 | -1.41~+4.90 |

Sewage sludge (SS); Waste glass (WG)

SSRSAs was -14.80 to -18.33% (shrinkage) and -6.37 to -8.20% (shrinkage). At 1100°C, particle size of SSRSAs shrank due to volatilization of organic matter, as well as the sintering effect; however, at 1150°C, although the SSRSA expanded, due to the volatilization of organic matter to result in particle size shrinkage, the particle size shrinks eventually. At 1100°C, the WGRSAs had already been sintered and caused particle shrinkage. At 1150°C, particle size increased due to expansion of aggregates.

The weight losses of both SSRSAs and WGRSAs were positively correlated with sintering temperatures. Of which, the correlation in SSRSAs is more significant. Its weight losses ranged from 16.33–18.45%, which are 3 or 4 times more than those of WGRSAs.

At 1100°C and 1150°C, the change rate in unit weight of a single particle of SSRSAs were 36.49–52.63% (*i.e.*, increase) and -1.41–4.90%, respectively. The change rate in unit weight of a single particle of WGRSAs was 3.36–9.52% (*i.e.*, increase) and from -19.77 to -21.66% (*i.e.*, reduction). The foresaid results show that the sintering behavior of WGRSAs was significantly different from that of the SSRSAs because the SSRSAs had a greater weight loss than the WGRSAs; however, the particle size reduction of WGRSAs was more significant than its weight loss. Therefore, during sintering, the WGRSAs have better lightweight characteristics than SSRSAs.

3.4 Dry specific gravity, water absorption and weight loss during sintering of reservoir-sediment aggregates

At 1050–1150°C, the dry specific gravities of PRSAs ranged between 1.97–2.49, and their dry specific gravities reduced to 1.58, which met the lightweight aggregate criteria, when the temperature reached to 1200°C. At 1050°C, 1100°C, 1150°C, and 1200°C, the dry specific gravity of SSRSAs was 2.24, 2.09, 1.74, and 1.36, respectively; and the specific gravity of WGRSAs was 2.37, 1.82, 1.50, and 1.09, respectively. The dry specific gravity of the WGRSAs and SSRSAs decreased following the increase of sintering temperature (Table 5 and Fig. 4). Taking the dry specific gravity of PRSAs as a benchmark, the dry specific gravity of WGRSAs and SSRSAs could reduce by 10.55%, 2.18%, and 17.09% at 1100°C, 1150°C, and 1200°C, respectively. It

Table 5 Characteristics of the reservoir-sediment aggregates

| Temperature (°C) | Proportions | Dry specific gravity | Water absorption (for 24h) (%) | Mohr hardness | Failure point loading (kgf) | Weight change after sinter (%) | Chemical corrosion resistance (%) | | Potential alkali-silica reactivity, Sc/Rc |
|------------------|-------------|----------------------|--------------------------------|---------------|-----------------------------|--------------------------------|-----------------------------------|---------------------------------|---|
| | | | | | | | 1.5N NaOH solution | 0.54N HNO ₃ solution | |
| 1050 | RS100 | 2.49 | 7.98 | 6 | 198.8 ± 65.5 | 6.67 | 0.16 | 0.19 | 0.37 |
| | RS80SS20 | 2.24 | 17.09 | 4 | 82.4 ± 17.7 | 18.88 | 0.07 | 0.26 | 0.17 |
| | RS80WG20 | 2.37 | 2.20 | 7 | 285.5 ± 44.6 | 5.16 | 0.07 | 0.20 | 0.41 |
| 1100 | RS100 | 2.56 | 1.60 | 6 | 372.4 ± 67.9 | 9.25 | 0.14 | 0.15 | 0.22 |
| | RS80SS20 | 2.09 | 1.17 | 8 | 231.6 ± 77.3 | 25.60 | 0.03 | 0.12 | 0.25 |
| | RS80WG20 | 1.82 | 0.96 | 9 | 180.1 ± 33.6 | 5.20 | 0.13 | 0.14 | 0.41 |
| 1150 | RS100 | 1.97 | 0.74 | 6 | 173.7 ± 76.8 | 6.80 | 0.11 | 0.14 | 0.21 |
| | RS80SS20 | 1.74 | 0.27 | 7 | 144.1 ± 38.7 | 18.86 | 0.16 | 0.16 | 0.26 |
| | RS80WG20 | 1.50 | 0.24 | 9 | 121.9 ± 24.5 | 5.15 | 0.12 | 0.16 | 0.38 |
| 1200 | RS100 | 1.58 | 0.92 | 7 | 145.2 ± 23.4 | 6.88 | 0.12 | 0.15 | 0.29 |
| | RS80SS20 | 1.36 | 0.78 | 8 | 104.0 ± 17.9 | 18.98 | 0.04 | 0.12 | 0.16 |
| | RS80WG20 | 1.09 | 1.10 | 9 | 55.3 ± 15.8 | 4.99 | 0.11 | 0.15 | 0.31 |

Reservoir sediment (RS); Sewage sludge (SS); Waste glass (WG); Sc(mmols/L), Rc(mmols/L)

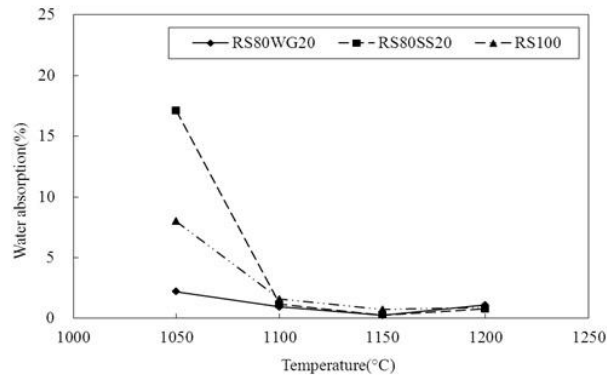


Fig. 5 Water absorption of reservoir-sediment aggregates

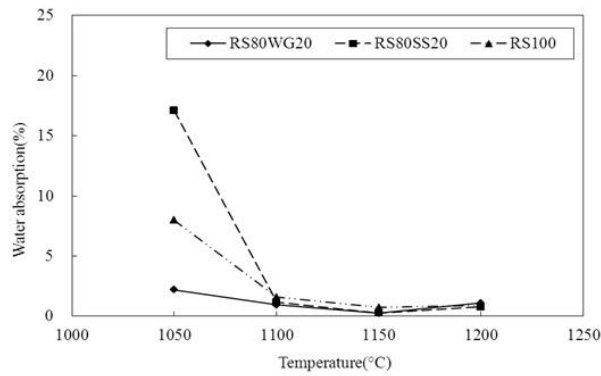


Fig. 6 Failure point loading of reservoir-sediment aggregates

indicated that WGRSAs was lighter than SSRSAs, and the dry specific gravity of WGRSAs would reduce more significantly than that of SSRSAs with the increase of sintering temperature.

At 1050–1150°C, water absorptions of the various aggregates decreased as sintering temperature increased. At 1100°C, water absorptions of the various aggregates were all less 1.60%; however, at 1200°C, water absorptions of all aggregates slightly improved because all aggregates had expanded significantly (Fig. 5). At 1050°C, the water absorption of PRSAs, SSRASs, and WGRSAs was 7.98%, 17.09%, and 2.20%, respectively, because the melting point of RS (about 1150–1200°C) was significantly higher than that of WG (about 1050–1100°C). Therefore, RS had not yet reached its melting point and had difficulty filling pores; however, SS became porous due to its decomposition of organic matters.

At 1050–1200°C, the weight losses of PRSAs, SSRSAs, and WGRSAs were 6.67–9.25%, 8.86–25.60%, and 4.99–5.20% respectively. Of which, the weight loss of SSRSAs was the highest. This demonstrated that the tendency of weight loss of RSAs during sintering was consistent with that of water absorption.

3.5 Failure point loading and hardness of reservoir-sediment aggregates

The particle sizes of the reservoir-sediment aggregates used in this study are similar and their shapes are almost spherical. 10 pellets of reservoir-sediment aggregates were randomly picked from each mixing proportion and proceeded the failure point loading test. The average failure point loading of PRSAs, WGRSAs, and SSRSAs was 145.2–372.4kgf, 82.4–231.6kgf, and 55.3–285.5kgf, respectively (Table 5). At 1100–1200°C, sintering temperature was in a negative relationship with the failure point loading of aggregates (Fig. 6). The PRSAs had the highest failure point loading, followed by that of SSRSAs and WGRSAs. At 1050°C, PRSAs had not yet been sintered. Test results for specific gravity, water absorption, and failure point loading indicated that the optimum sintering temperature for the PRSAs, SSRSAs, and WGRSAs was 1150°C, 1100°C, and 1050°C, respectively, and at this temperature, the various aggregates had glassy surfaces.

Mohr hardness for the PRSAs, WGRSAs, and SSRSAs was 6–7, 7–8, and 8–9 at 1100–1200°C (Table 5). The foresaid results of failure point loading and hardness showed that PRSAs had superior toughness, followed by that of SSRSAs. On the contrary, WGRSAs were brittle.

3.6 Chemical stability of reservoir-sediment aggregates

In this study, the chemical stability of aggregates was investigated through the chemical corrosion resistance, chemical soundness and potential alkali-silica reactivity. The aggregates were immersed into two solutions (1.5N sodium hydroxide solution, and 0.54N nitric acid solution) to perform the chemical stability test. The aggregates were heated in the solutions of 80°C respectively, and immersed for two hours to measure the weight loss of the aggregates. As to the chemical corrosion resistance in acids and alkaline solutions, when immersed in a nitric acid solution, the weight loss of PRSAs, SSRSAs, and WGRSAs was 0.14–0.19%, 0.12–0.26%, and 0.12–0.20% respectively; when immersed in a sodium hydroxide solution, the weight loss was 0.11–0.16%, 0.03–0.16%, and 0.07–0.13%, respectively (Table 5). These measurement results indicated that WGRSAs was superior to SSRSAs in chemical corrosion resistance.

The weight loss on chemical soundness test (MgSO₄ solution) of PRSAs, SSRSAs and

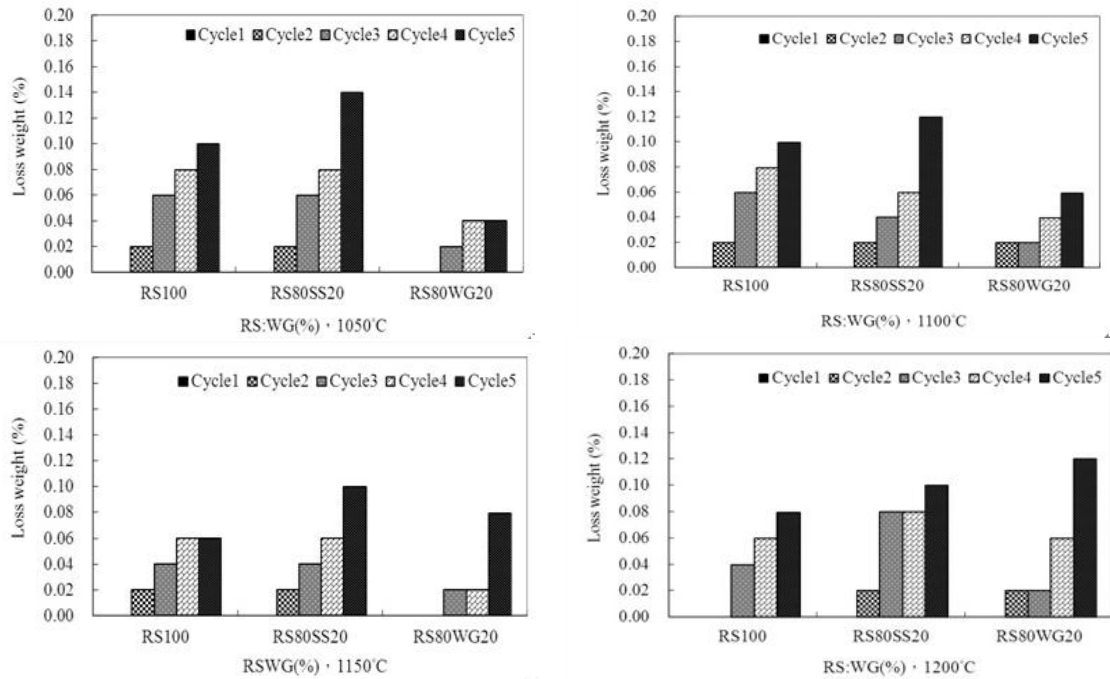


Fig. 7 Chemical soundness of reservoir-sediment aggregates ($MgSO_4$ solution)

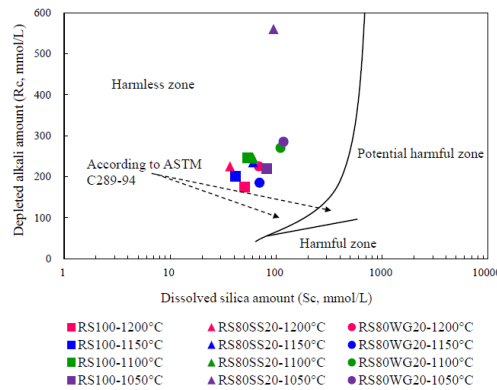


Fig. 8 Potential alkali- silica reactivity of reservoir-sediment aggregates

WGRSAs was 0.6–0.10%, 0.10–0.14%, and 0.04–0.12% respectively. With the increase of sintering temperature, the weight loss of aggregates all decreased (Fig. 7). The WGRSAs was better than the SSRSAs in chemical soundness.

ASTM C289-94 was adopted. The potential alkali-silica reactivity of RS aggregates was evaluated using the Chemical Method Judgment Chart based on the amount of dissolved silica (Sc) and amount of depleted alkali (Rc). Table 5 shows that the Sc/Rc ratio in PRSAs, SSRSAs, and WGRSAs was 0.21–0.37, 0.16–0.26, and 0.31–0.41, respectively, all far below 1.0. This demonstrated that PRSAs, SSRSAs, and WGRSAs were all harmless in potential alkali-silica reactivity (Fig. 8).

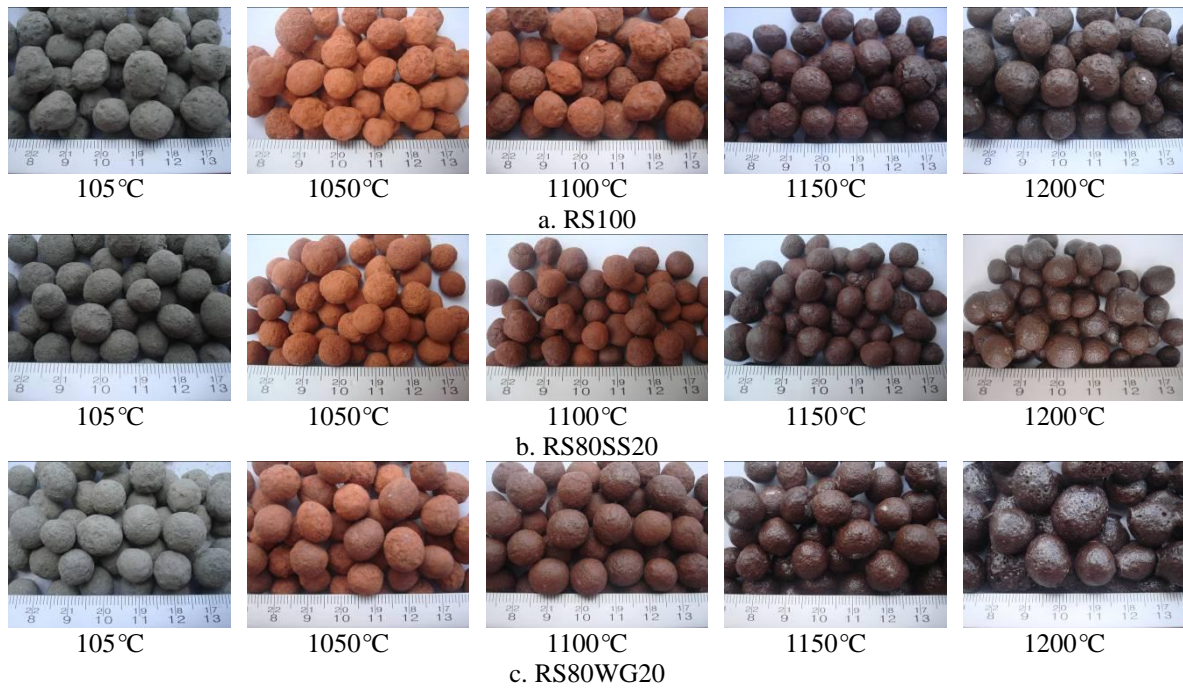


Fig. 9 Appearances of reservoir-sediment aggregates

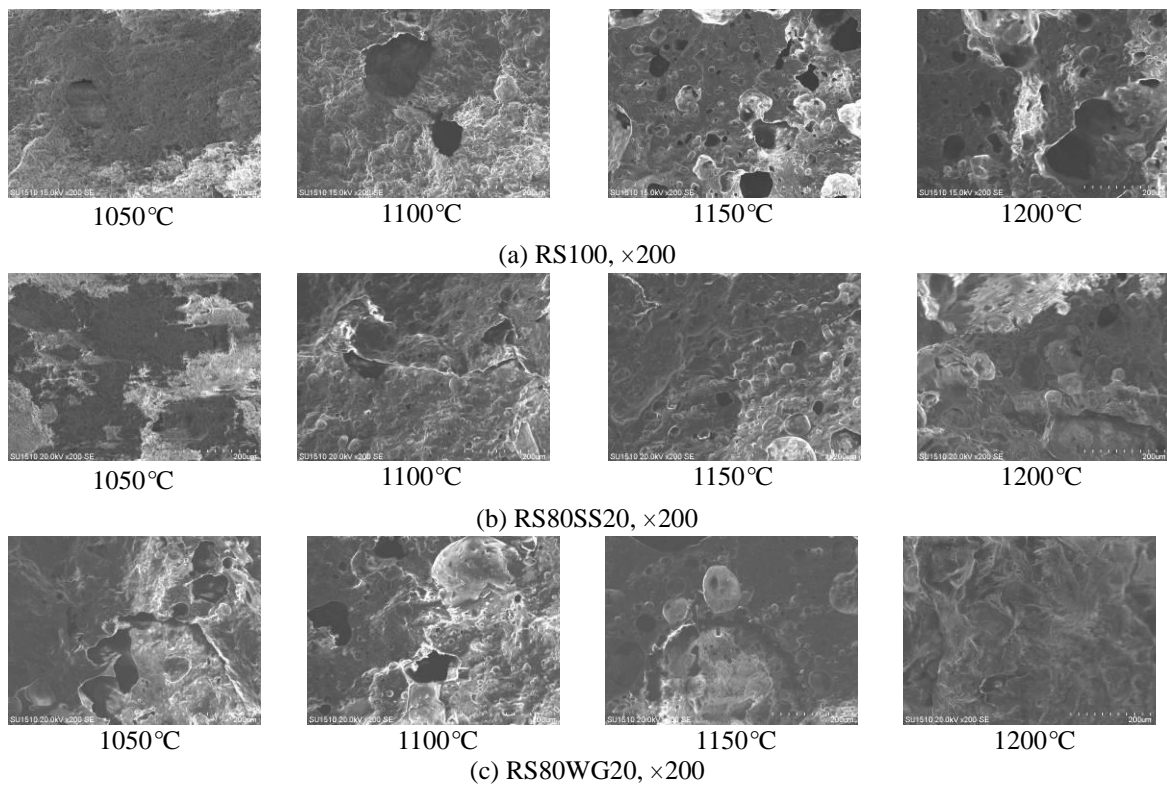


Fig. 10 SEM microstructures of reservoir-sediment aggregates

3.7 Appearance and microscopic images of reservoir-sediment aggregates

Fig. 9 shows the change in particle size of RSAs before and after sintering. At 1050°C, the SSRSAs were typically reddish brown (Fe_2O_3) and had an incomplete sintered surface—its surface had residual powders. At 1100°C, the SSRSAs turned beige, and had a completely sintered surface. The aggregates turned deep brown (Fe_3O_4) at 1150–1200°C, and at 1200°C, the surface of aggregates was very glossy. At 1050°C, as the amount of WG increased, the WGRSAs were dark red-brown, and the surface was sintered more completely than that of SSRSAs, and only little amount of powder remained on the aggregate's surface. At 1100°C, the aggregate turned light brown and its surface was sintered because WG had a low melting point. At 1150–1200°C, the surface of aggregates was very glossy and when the temperature was up to 1200°C, aggregates expanded significantly.

Fig. 10 shows an SEM image at 200X magnification. At 1150–1200°C, melt flow phenomenon of PRSAs was visible and PRSAs became porous due to the foaming effect. The pores in the micro-structures of SSRSAs generally increased as sintering temperature increased, but the pore size was significantly smaller than that of the PRSAs; at 1050°C, pores in aggregates decreased and scattered unevenly because 1050°C was lower than the required sintering temperature. At 1150°C, small pores in aggregate's micro-structures gradually increased; at this moment, the aggregate's specific gravity was $1.74\text{g}/\text{cm}^3$, meeting the standard of lightweight aggregates. At 1200°C, the aggregate's pores increased significantly in both number and size. At 1050–1100°C, glass-phase substances were formed in WGRSAs to fill pores in micro-structures and make the aggregates densified; at this moment, the aggregate's micro-structure was glossy and pores scattered evenly. At 1150–1200°C, huge amount of glass-phase substances were formed in WGRSAs, and most of the gases were coated within aggregates to make the aggregates expanded apparently.

4. Conclusions

- The lightweight characteristics of WGRSAs are more significant than those of SSRSAs. Moreover, as sintering temperature increases, the specific gravity of WGRSAs drops more apparently.
- Test results for specific gravity, water absorption, and failure point loading indicated that the optimum sintering temperature for the PRSAs, SSRSAs, and WGRSAs was 1150°C, 1100°C, and 1050°C, respectively.
- PRSAs had superior toughness, followed by that of SSRSAs. On the contrary, WGRSAs were brittle.
- At 1100°C and 1150°C, the change rate in particle size of WGRSAs was -3.79 to -4.65% (shrinkage) and 5.68 to 6.30% (expansion) respectively; while the change rate in particle size of SSRSAs was -14.80 to -18.33% (shrinkage) and -6.37 to -8.20% (shrinkage).
- The PRSAs are normal weight with better strength; the WGRSAs are lightweight and energy-saving; and the SSRSAs are lightweight with normal strength.

References

- ASTM C289-94 (2000), *Standard Test Method for Potential Alkali-Silica Reactivity of Aggregates (Chemical Method)*, Annual Book of ASTM Standards, Philadelphia, UAS.

- Bernardo, E., Bonomo, E. and Dattoli, A. (2010), "Optimisation of sintered glass-ceramics from an industrial waste glass", *Ceramics Int.*, **36**, 1675-1680.
- Chiou, I.J. and Chen, C.H. (2013), "Effects of waste glass fineness on the sintering behavior of reservoir sediment aggregates", *Constr. Build. Mater.*, **38**, 987-993.
- Chiou, I.J., Wang, K.S., Chen, C.H. and Lin, Y.T. (2006), "Lightweight aggregate made from sewage sludge and incinerated ash", *Waste Manage.*, **26**(12), 1453-1461.
- Cheeseman, C.R. and Viridi, C.R. (2005), "Properties and microstructure of lightweight aggregate produced from sintered sewage sludge ash", *Resour. Conserv. Recy.*, **45**, 18-30.
- Chiou, I.J. and Chen, C.H. (2011), "Properties of artificial aggregates made from waste sludge", *Comput. Concr.* **8**(6), 617-629.
- Corinaldesi, V., Gnappi, G., Moriconi, G. and Montenero, A. (2005), "Reuse of ground waste glass as aggregate for mortars", *Waste Manage.*, **25**, 197-201.
- Chen, H.J., Yang, M.D., Tang, C.W. and Wang, S.Y. (2012), "Producing synthetic lightweight aggregates from reservoir sediments", *Constr. Build. Mater.*, **28**, 387-394.
- Hung, M.F. and Hwang, C.L. (2007), "Study of fine sediments for making lightweight aggregate", *Waste Manage. Res.*, **25**, 449-456.
- Ismail, Z.Z., AL-Hashmi, E.A., (2009), "Recycling of waste glass as a partial replacement for fine aggregate in concrete", *Waste Manage. Res.*, **29**, 655-659.
- Khan, M. and Scullion, J. (2002), "Effects of metal (Cd, Cu, Ni, Pb or Zn) enrichment of sewage-sludge on soil micro-organisms and their activities", *Appl. Soil Ecology.*, **20**, 145-155.
- Lee, M.Y., Ko, C.H., Chang, F.C., Lo, S.L., Lin, J.D., Shan, M.Y. and Lee, J.C. (2008), "Artificial stone slab production using waste glass, stone fragments and vacuum vibratory compaction", *Cement Concrete Compos.*, **30**, 583-587.
- Lee, G., Ling, T.C., Wong Y.L. and Poon, C.S. (2011), "Effects of crushed glass cullet sizes, casting methods and pozzolanic materials on ASR of concrete blocks", *Constr. Build. Mater.*, **25**, 2611-2618.
- Lin, K.L., Huang, W.J., Shie, J.L., Lee, T. C., Wang, K.S. and Lee, C.H. (2009), "The utilization of thin film transistor liquid crystal display waste glass as a pozzolanic material", *J. Hazard. Mater.*, **163**, 916-921.
- Mun, K.J. (2007), "Development and tests of lightweight aggregate using sewage sludge for nonstructural concrete", *Constr. Build. Mater.*, **21**, 1583-1588.
- Park, S.B., Lee, B.C. and Kim, J.H. (2004), "Studies on mechanical properties of concrete containing waste glass aggregate", *Cement Concrete Res.*, **34**, 2181-2189.
- Qi, Y.F., Yue, Q., Han, S., Yue, M., Gao, B., Yu, H. and Shao, T. (2010), "Preparation and mechanism of ultra-lightweight ceramics produced from sewage sludge", *J. Hazard. Mater.*, **176**, 76-84.
- Singh, R.P. and Agrawal, M. (2008), "Potential benefits and risks of land application of sewage sludge", *Waste Manag.*, **28**, 347-358.
- Su'ha Yu'ru'yen and H.O' zkan Toplan. (2009), "The sintering kinetics of porcelain bodies made from waste glass and fly ash", *Ceramics Int.*, **35**, 2427-2433.
- Terro, M.J. (2006), "Properties of concrete made with recycled crushed glass at elevated temperatures", *Build. Environ.*, **41**, 633-639.
- Tsai, C.C., Wang, K.S. and Chiou, I.J. (2006), "Effect of SiO₂-Al₂O₃-flux ratio change on the bloating characteristics of lightweight aggregate material produced from recycled sewage sludge", *J. Hazard. Mater.*, **134**, 87-93.
- Tang, C.W., Chen C.W., Wang, S.Y. and Spaulding, J. (2011), "Production of synthetic lightweight aggregate using reservoir sediments for concrete and masonry", *Cement Concrete Compos.*, **33**, 292-300.
- Vu, D.H., Wang, K.S. and Bac, B.H. (2011), "Humidity control porous ceramics prepared from waste and porous materials", *Mater. Letts.*, **65**, 940-943.
- Wang, K.S., Chiou, I.J., Chen, C.H. and Wang, D. (2005), "Lightweight properties and pore structure of foamed material made from sewage sludge ash", *Constr. Build. Mater.*, **19**, 627-633.
- Wang, X., Jin, Y., Wang, Z., Nie, Y.F., Huang, Q. And Wang, Q. (2009), "Development of lightweight aggregate from dry sewage sludge and coal ash", *Waste Manage.*, **29**, 1330-1335.
- Wang, H.Y. and Sheen Y.N. (2010), "Performance characteristics of dredged silt and high-performance

- lightweight aggregate concrete”, *Comput. Concr.*, **7**(1), 53-62.
- Wei, Y.L., Lin, C.Y., Ko, K.W. and Wang, H.P. (2011), “Preparation of low water-sorption lightweight aggregates from harbor sediment added with waste glass”, *Mar. Pollut. Bull.*, **63**, 5-12.
- Zhang, W.Y., Gao, H. and Xub, Y. (2011), “Sintering and reactive crystal growth of diopside–albite glass–ceramics from waste glass”, *J. European Ceramic Societ.*, **31**, 1669-1675.

CC